

## Research Article

### Microfabrication through Electrostatic Self-Assembly

Joe Tien, Andreas Terfort, and George M. Whitesides

*Langmuir*, 1997, 13 (20), 5349-5355 • DOI: 10.1021/la970454i

Downloaded from <http://pubs.acs.org> on January 15, 2009

#### More About This Article

---

Additional resources and features associated with this article are available within the HTML version:

- Supporting Information
- Links to the 14 articles that cite this article, as of the time of this article download
- Access to high resolution figures
- Links to articles and content related to this article
- Copyright permission to reproduce figures and/or text from this article

[View the Full Text HTML](#)



**ACS Publications**  
High quality. High impact.

# Microfabrication through Electrostatic Self-Assembly

Joe Tien, Andreas Terfort, and George M. Whitesides\*

Department of Chemistry and Chemical Biology, Harvard University,  
Cambridge, Massachusetts 02138

Received May 2, 1997. In Final Form: July 29, 1997<sup>⊗</sup>

We use electrostatic interactions to direct the patterning of gold disks having  $\sim 10\text{-}\mu\text{m}$  diameters on functionalized surfaces. Planar and curved substrates with patterned surface charge were generated either by microcontact printing or by photolithography. Small charged gold disks were generated by electroplating gold into photoresist molds and derivatizing these disks with charged self-assembled monolayers. When agitated as a suspension in contact with the patterned surfaces, the charged gold disks deposited specifically but as disordered aggregates on regions presenting the opposite charge. Positively-charged disks deposited on phosphonate-, carboxylate-, and SiOH-terminated surfaces but not on trimethylammonium- and dimethylammonium-terminated surfaces, and vice versa for negatively-charged disks. Methyl- and  $\text{CF}_3$ -terminated surfaces resisted deposition of disks of either charge. Selective and dense assembly was achieved in methanol, ethanol, 2-propanol, and dioxane; in water, deposition was nonspecific. The overlap of disks was eliminated by using disks with  $\sim 1:1$  aspect ratios.

## Introduction

Self-assembly has emerged as a useful strategy for assembling molecular components into complex aggregates.<sup>1–4</sup> Extending self-assembly to larger components, such as colloids<sup>5,6</sup> and micrometer-scale objects,<sup>7</sup> is just beginning, and our prior work in this area has relied on capillary forces to drive the assembly.<sup>8,9</sup> This paper demonstrates the use of *electrostatic* interactions to direct the patterning of surfaces with disks having  $\sim 10\text{-}\mu\text{m}$  diameters.

The basic principle of this technique is straightforward: Two oppositely charged particles, suspended in a fluid, will attract. Electrostatic interactions have a longer range than hydrophobic or hydrogen-bonding interactions,<sup>10,11</sup> and assemblies formed electrostatically can, in principle, form by attraction of particles over substantial distances. We found it most convenient to generate charged microstructures using self-assembled monolayers (SAMs). By electroplating gold into cavities of patterned photoresist, releasing the gold into ethanol, and modifying the surfaces with charged alkanethiols, we obtained charged gold particles with well-defined shapes; various sizes and shapes could be fashioned by altering the photoresist pattern. When stirred in suspension with a surface patterned with charged SAMs, the charged gold

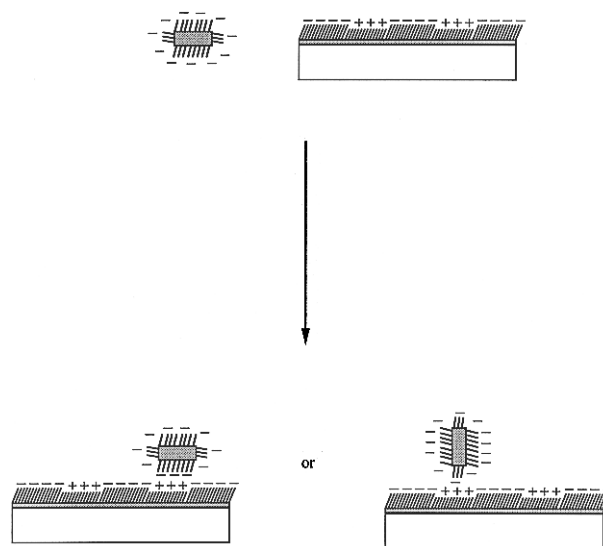


**Figure 1.** Schematic description of electrostatic self-assembly. A charged object deposits onto an oppositely charged surface through electrostatic attraction. Charges are provided by appropriately functionalized SAMs.

particles selectively attached to regions presenting the opposite charge (Figure 1).

## Methods

Self-assembly through electrostatic interactions consisted of the preparation of a charged surface, the fabrication of charged microstructures, and the assembly of these microstructures onto the surface (Figure 2).

**Preparation of Charged Surfaces.** Substrates with a uniform surface charge were made by immersing clean gold surfaces in a 1 mM ethanolic solution of alkanethiol for  $\sim 10$  min. Derivatization with  $\text{HS}(\text{CH}_2)_{11}\text{NH}_3^+\text{Cl}^-$ ,  $\text{HS}(\text{CH}_2)_{11}\text{NMe}_2$ ,  $\text{HS}(\text{CH}_2)_{11}\text{NMe}_3^+\text{Br}^-$ , or  $\text{HS}(\text{CH}_2)_{11}\text{C}(\text{NH}_2)_2^+\text{Cl}^-$  yielded positively-charged surfaces, with  $\text{HS}(\text{CH}_2)_{15}\text{COOH}$  and  $\text{HS}(\text{CH}_2)_{11}\text{PO}_3\text{H}_2$  yielding negatively-charged surfaces. Gold substrates with zero surface charge were made by immersion of clean gold films in 1 mMethanolic solution of  $\text{HS}(\text{CH}_2)_{15}\text{CH}_3$  or  $\text{HS}(\text{CH}_2)_2(\text{CF}_2)_5\text{CF}_3$ . We also used a clean silicon surface with native oxide as a negatively-charged surface (the surface Si–OH groups<sup>12</sup> have  $\text{p}K_a \approx 2\text{--}4$  and are extensively ionized in water at pH 7) and an HF-treated hydrogen-terminated

<sup>⊗</sup> Abstract published in *Advance ACS Abstracts*, September 15, 1997.

(1) Whitesides, G. M.; Zerkowski, J. A.; MacDonald, J. C.; Chin, D. *Mater. Res. Soc. Symp. Proc.* **1994**, *328*, 3–13.

(2) Hartgerink, J. D.; Granja, J. R.; Milligan, R. A.; Ghadiri, M. R. *J. Am. Chem. Soc.* **1996**, *118*, 43–50.

(3) Tjivikua, T.; Ballester, P.; J. Rebek, J. *J. Am. Chem. Soc.* **1990**, *112*, 1249–1250.

(4) Simanek, E. E.; Li, X.; Choi, I. S.; Whitesides, G. M. In *Templating, Self-Assembly, and Self-Organization*; Sauvage, J.-P., Hosseini, M. W., Eds.; Elsevier Science: Oxford, 1996; Vol. 9.

(5) Colvin, V. L.; Goldstein, A. N.; Alivisatos, A. P. *J. Am. Chem. Soc.* **1992**, *114*, 5221–5230.

(6) Murray, C. B.; Kagan, C. R.; Bawendi, M. G. *Science* **1995**, *270*, 1335–1338.

(7) Verma, A. K.; Hadley, M. A.; Yeh, H.-J. J.; Smith, J. S. 45th Electronic Components and Technology Conference, Las Vegas, NV, 1995; pp 1263–1268.

(8) Terfort, A.; Bowden, N.; Whitesides, G. M. *Nature* **1997**, *386*, 162–164.

(9) Bowden, N.; Terfort, A.; Carbeck, J.; Whitesides, G. M. *Science* **1997**, *276*, 233–235.

(10) Krupp, H. *Adv. Colloid Interface Sci.* **1967**, *1*, 111–239.

(11) Maboudian, R.; Howe, R. T. *J. Vac. Sci. Technol., B* **1997**, *15*, 1–20.

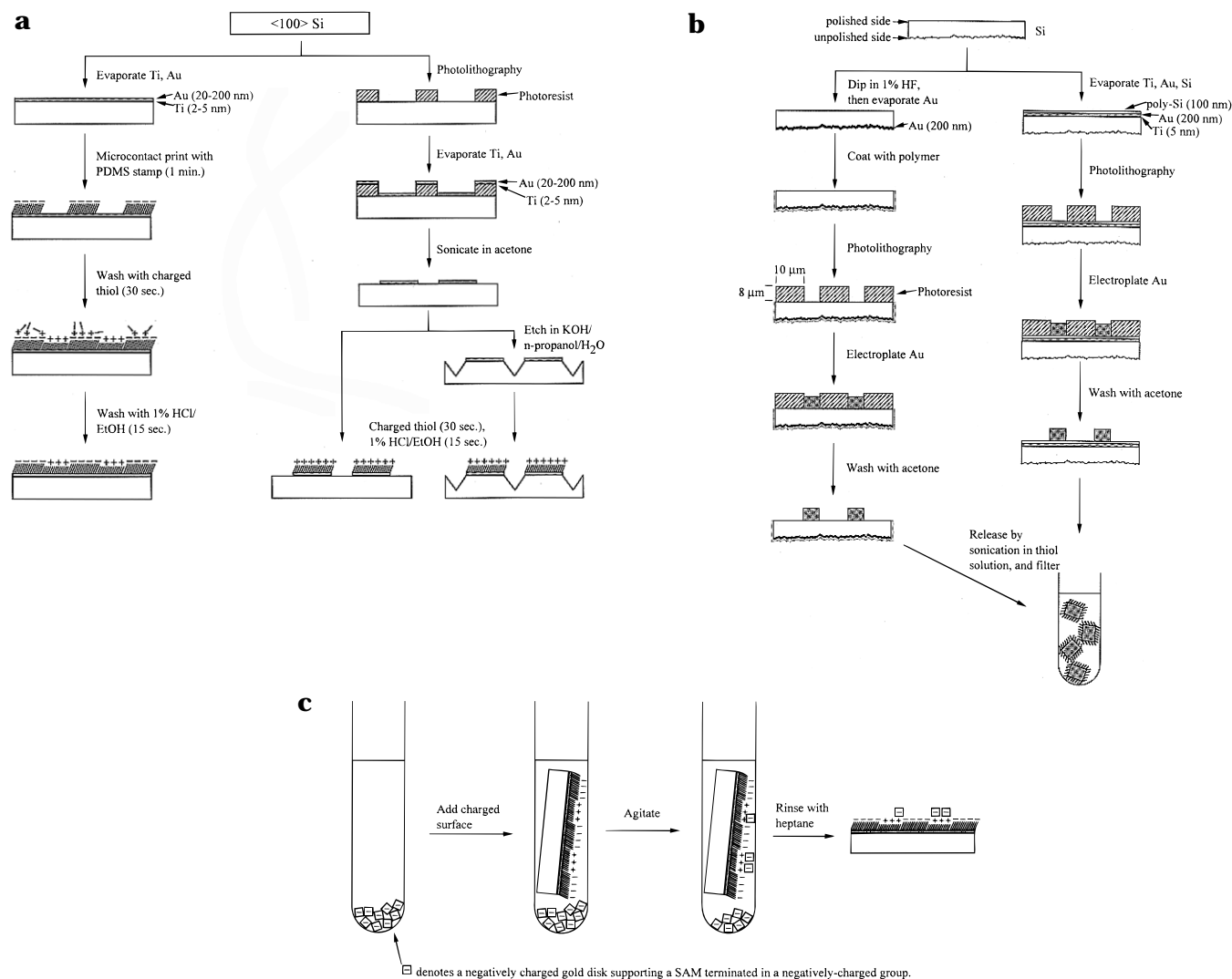


**Figure 2.** Diagram of experimental methods: (a) fabrication of patterned surfaces; (b) fabrication of charged gold microstructures; (c) assembly of particles.

silicon surface as a neutral surface (with 1–5% residual Si–OH groups<sup>13</sup>).

Surfaces with patterned charge were fabricated by microcontact printing, liftoff, or etching (Figure 2a). Substrates patterned by microcontact printing<sup>14</sup> were made by stamping a gold film for 1 min with a poly-(dimethylsiloxane) stamp inked with HS(CH<sub>2</sub>)<sub>15</sub>CH<sub>3</sub> or HS(CH<sub>2</sub>)<sub>15</sub>COOH, washing for 30 sec with a 1 mM ethanolic solution of charged thiol, and washing for 15 s with 1% HCl/EtOH to remove any electrostatically bound material.

Patterned surfaces by liftoff or etching were made by evaporating gold onto patterned photoresist on <100> silicon. Sonication in acetone dissolved the resist to reveal silicon/gold patterns, some of which were etched in a mixture containing 270 mL of H<sub>2</sub>O, 80 mL of 1-propanol, and 80 g of KOH at 70–80 °C to generate silicon grooves with gold-topped mesas. The gold regions on both the etched and unetched wafers were subsequently derivatized by washing with charged thiol solution and 1% HCl/EtOH.

**Fabrication of Charged Gold Microstructures.** Gold disks were fabricated by electrodeposition in a

photoresist mold. Our strategy was to electroplate gold directly on a silicon surface and to rely on weak adhesion between gold and silicon to enable subsequent removal of the gold particles. This approach required that the cathodes consist of a metallic surface sandwiched between an insulator and the silicon surface (Figure 2b). The silicon wafers we used had a sufficient high resistivity that plating without embedded electrodes resulted in nonuniform electrodeposition. Cathodes were made by evaporating 200 nm of gold onto the rough *backside* of hydrogen-terminated silicon wafers and curing a thin film of polyurethane (Norland Optical Adhesive 88) onto the gold or by evaporating 200 nm of gold, followed by 50–100 nm of silicon, onto the smooth side of an oxidized silicon wafer. The cathodes were patterned with photoresist, washed with 1% aqueous HF (with a few drops of Triton X-100 to enhance wetting) to remove any native silicon oxide, and plated to deposit gold in regions not masked by photoresist. A 5 cm × 5 cm platinum sheet served as the anode. Following plating, the cathodes were rinsed with acetone to remove the photoresist and sonicated in a beaker of charged thiol solution: Sonication separated the plated gold disks and allowed a SAM to form as their surfaces. The resulting suspension of SAM-covered disks was filtered through a 20-μm nylon mesh and left under thiol solution for several hours. Once the charged SAM had formed, these gold disks could be further coated with an

(12) Parks, G. A. *Chem. Rev.* **1965**, *65*, 177–198.

(13) Wong, C. Y.; Klepner, S. P. *Appl. Phys. Lett.* **1986**, *48*, 1229.

(14) Kumar, A.; Biebuyck, H. A.; Whitesides, G. M. *Langmuir* **1994**, *10*, 1498–1511.

**Table 1. Classification of Surfaces**

nonstick	(+) attracting	(-) attracting	sticky
CH <sub>3</sub> -terminated SAM CF <sub>3</sub> -terminated SAM	H-terminated Si (Si-H) <sup>a</sup> CO <sub>2</sub> H <sup>-</sup> -terminated SAM PO <sub>3</sub> H <sup>-</sup> -terminated SAM hexaethylene glycol-terminated SAM oxidized Si (Si-O <sup>-</sup> )	NMe <sub>3</sub> <sup>+</sup> -terminated SAM C(NH <sub>2</sub> ) <sub>2</sub> <sup>+</sup> -terminated SAM NH <sub>3</sub> <sup>+</sup> -terminated SAM NMe <sub>2</sub> H <sup>+</sup> -terminated SAM	bare gold

"nonstick" surfaces resist both (+)-charged and (-)-charged disks

"(+)-attracting" surfaces attract (+)-charged disks and resist (-)-charged disks

"(-)-attracting" surfaces resist (+)-charged disks and attract (-)-charged disks

"sticky" surfaces attract both (+)-charged and (-)-charged disks

<sup>a</sup> The H-terminated surface is not completely passivated after an HF treatment.<sup>13</sup>

oppositely charged polymer (hexadimethrine bromide for negatively-charged gold, sodium poly(vinylsulfonate) for positively-charged gold) by immersion in a 20 mM aqueous solution of the polymer for 10–30 min.<sup>15</sup>

#### Assembly of Charged Particles onto Surfaces.

Gold particles covered with an ionized SAM were placed in a glass test tube with approximately 3 mL of solvent; the ionized SAM stabilized the gold particles against aggregation (Figure 2c). Wafers with patterned surface charge were cut into 0.5-cm × 3-cm pieces and placed in the same test tube. The test tube was then agitated to suspend the gold particles and reagitated whenever the particles settled. After a few minutes, the wafer, along with any attached gold particles, was carefully removed from the test tube, placed in a dish of heptane, and removed from heptane and allowed to dry. (The treatment with heptane reduces capillary forces after removal from solvent.)

## Results and Discussion

**Classification of Surfaces.** We label a surface *nonstick* if it resisted the deposition of both positively- and negatively-charged particles, *attractive/repulsive* if particles of one charge deposited and those of the opposite charge did not, and *sticky* if particles of both charges deposited (Table 1). By "negatively-charged", we mean PO<sub>3</sub>H<sup>-</sup>-terminated, CO<sub>2</sub><sup>-</sup>-terminated, and poly(vinylsulfonate)-coated gold particles. "Positively-charged" particles included gold covered with NMe<sub>2</sub>-terminated SAMs (existing, we presume, at least in part as NMe<sub>2</sub>H<sup>+</sup> in contact with a protic solvent), with NMe<sub>3</sub><sup>+</sup>-terminated SAMs, or with a layer of hexadimethrine bromide. (Gold disks covered with C(NH<sub>2</sub>)<sub>2</sub><sup>+</sup>-terminated or NH<sub>3</sub><sup>+</sup>-terminated SAMs assembled on every surface; i.e., *patterned* deposition of these particles was unsuccessful. We believe the formation of hydrophobic multilayers to be the cause.<sup>16</sup>) As expected, surfaces presenting a low free energy (Me-terminated and CF<sub>3</sub>-terminated SAMs) were nonstick toward deposition of disks, and charged surfaces were attractive to oppositely-charged disks and repulsive to disks of the same charge. The only sticky surface found was bare gold.

Two particular surfaces gave unexpected results: First, hydrogen-terminated silicon, although ostensibly a low-energy surface, attracted positively-charged particles. We attribute this result to the presence of residual Si–OH groups on the silicon. Second, hexaethylene glycol-terminated SAMs also attracted positively-charged particles, even though such SAMs are not charged. At this point, we are unsure why this assembly occurred.

Adhesion between adsorbed particles and a surface were strong enough to withstand shear hydrodynamic forces employed in the experiments. Sonication in water of a surface with adsorbed particles removed nearly all of the adsorbed shapes.

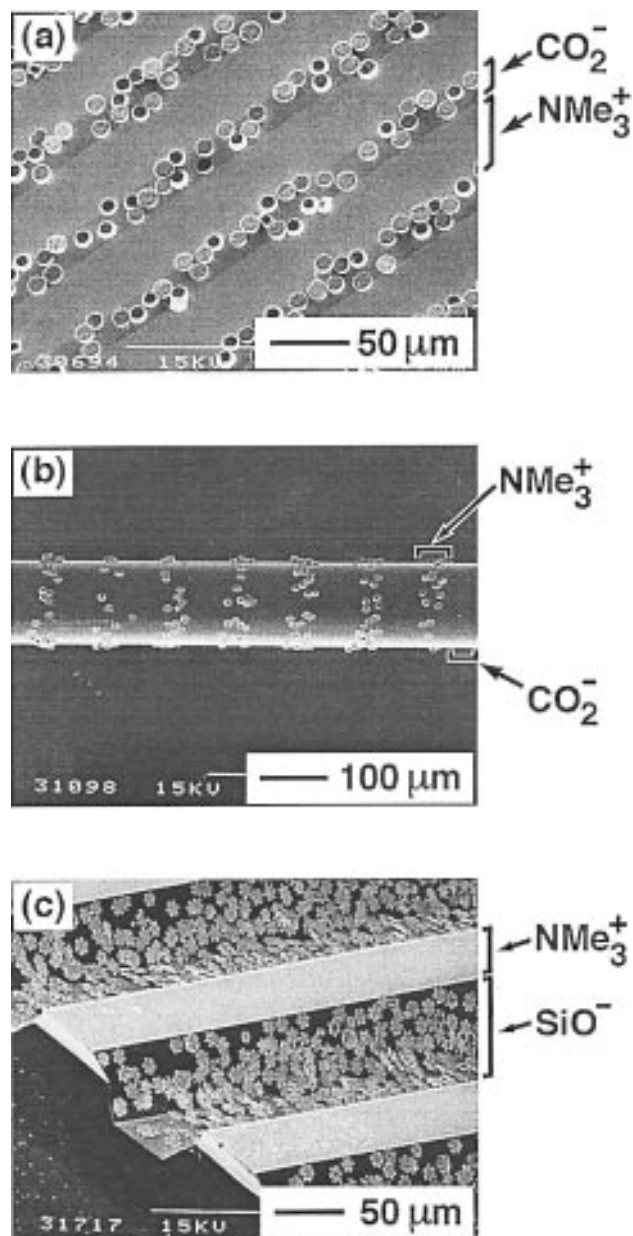
**Patterned Deposition of Gold Particles.** We judged the quality of the patterns by assuming that "ideal" assembly should cover attractive and sticky surfaces with an "expanded" monolayer of particles (due to electrostatic repulsion between adsorbed particles) while leaving nonstick and repelling surfaces bare, i.e., ideal assembly should be *selective* and *dense*. Figure 3 shows typical examples of "good" assemblies. Selectivity of deposition was found to be dependent on the choice of thiols and solvent used, while the density of deposition was affected by the geometry of the particles.

Figure 4 illustrates the effect of thiol used in micro-contact printing ( $\mu$ CP) on the selectivity of deposition. The gold wafer shown in Figure 4a was stamped with HS(CH<sub>2</sub>)<sub>15</sub>COOH, and that in Figure 4b, with HS(CH<sub>2</sub>)<sub>15</sub>-CH<sub>3</sub>; subsequent washing with HS(CH<sub>2</sub>)<sub>11</sub>NMe<sub>3</sub><sup>+</sup> and HCl/EtOH derivatized the unstamped regions. Deposition of PO<sub>3</sub>H<sup>-</sup>-terminated gold cylinders on the CO<sub>2</sub><sup>-</sup>/NMe<sub>3</sub><sup>+</sup> pattern was much more selective than that on the CH<sub>3</sub>/NMe<sub>3</sub><sup>+</sup> pattern, and there was extensive deposition on the CH<sub>3</sub>-terminated region. We believe that the deposition of PO<sub>3</sub>H<sup>-</sup>-terminated particles on the CH<sub>3</sub>-terminated surface is an artifact reflecting exchange of HS(CH<sub>2</sub>)<sub>11</sub>NMe<sub>3</sub><sup>+</sup> into the Me-terminated system during the preparation of the patterned surfaces (Figure 5). For the wafer patterned with CH<sub>3</sub>/NMe<sub>3</sub><sup>+</sup>, this contamination imparted a positive charge to the Me-terminated regions, which apparently was sufficient to attract PO<sub>3</sub>H<sup>-</sup>-terminated cylinders. As for the CO<sub>2</sub><sup>-</sup>/NMe<sub>3</sub><sup>+</sup> pattern, regions stamped with COOH-terminated thiol were still predominantly negatively charged and repelling. Thus, deposition on the CO<sub>2</sub><sup>-</sup>/NMe<sub>3</sub><sup>+</sup> pattern was highly selective, whereas deposition on the CH<sub>3</sub>/NMe<sub>3</sub><sup>+</sup> pattern was not.

Selectivity of deposition is also influenced by solvent, as shown in Figure 6: Assembly in ethanol was more selective than assembly from water. We believe the result to be a combination of two effects. First, hydrophobic effects are more pronounced in water than in ethanol and may compete with electrostatic interactions. Second, water is much more polar than ethanol and thus can screen any electrostatic interactions more strongly. Indeed, assembly from 1 M aqueous KBr, which shields electrostatic forces even more effectively than water, was not only unselective but not dense. Among other solvents, methanol, 2-propanol, and dioxane gave selective assemblies. Tetrahydrofuran, methylene chloride, chloroform, acetonitrile, and hexane all caused the gold particles to aggregate, rendering assembly impractical. Selective assembly seems to require a solvent with moderate polarity.

(15) Cheung, J. H.; Fou, A. F.; Rubner, M. F. *Thin Solid Films* **1994**, *244*, 985–989.

(16) Terfort, A.; Tien, J.; Whitesides, G. M. Unpublished results. Preliminary ellipsometry and contact angle measurements indicate that HS(CH<sub>2</sub>)<sub>11</sub>NH<sub>3</sub><sup>+</sup> and HS(CH<sub>2</sub>)<sub>10</sub>C(NH<sub>2</sub>)<sub>2</sub><sup>+</sup> form hydrophobic bilayers on gold, while HS(CH<sub>2</sub>)<sub>11</sub>NMe<sub>3</sub><sup>+</sup> and HS(CH<sub>2</sub>)<sub>11</sub>NMe<sub>2</sub> form monolayers.



**Figure 3.** SEMs of patterns of disks (or stars) after electrostatic self-assembly in ethanol: (a)  $\text{NMe}_3^+$ -terminated gold disks, assembled on gold surface patterned with  $\text{HS}(\text{CH}_2)_{15}\text{COOH}$  and  $\text{HS}(\text{CH}_2)_{11}\text{NMe}_3^+$ ; (b)  $\text{PO}_3\text{H}^-$ -terminated gold disks, assembled on a gold-covered capillary patterned with  $\text{HS}(\text{CH}_2)_{15}\text{COOH}$  and  $\text{HS}(\text{CH}_2)_{11}\text{NMe}_3^+$ ; (c) hexadimethrine bromide-coated gold stars, assembled in silicon grooves. The gold mesas were covered with  $\text{NMe}_3^+$ -terminated SAMs.

Figure 7 demonstrates the effect of particle aspect ratio on assembly. Here the selectivity of deposition is the same for either cylinders (1:1 aspect ratio) or disks (1:15). The flexibility of disks, however, allows for denser packing of particles through overlap.

### Conclusions

This paper describes the use of electrostatic interactions to pattern a surface with  $10\text{-}\mu\text{m}$ -sized gold particles. We have achieved selective adsorption of mesoscopic ( $\sim 10\text{-}\mu\text{m}$  diameter) particles on surfaces using electrostatic effects: (i) positively-charged gold particles deposited on  $\text{PO}_3\text{H}^-$ ,  $\text{CO}_2^-$ , and  $\text{SiO}^-$ -terminated surfaces but not on  $\text{NMe}_3^+$ - or  $\text{NMe}_2\text{H}^+$ -terminated surfaces; (ii) the reverse was true for negatively-charged gold particles; (iii) methyl- and  $\text{CF}_3$ -terminated surfaces resisted deposition of all

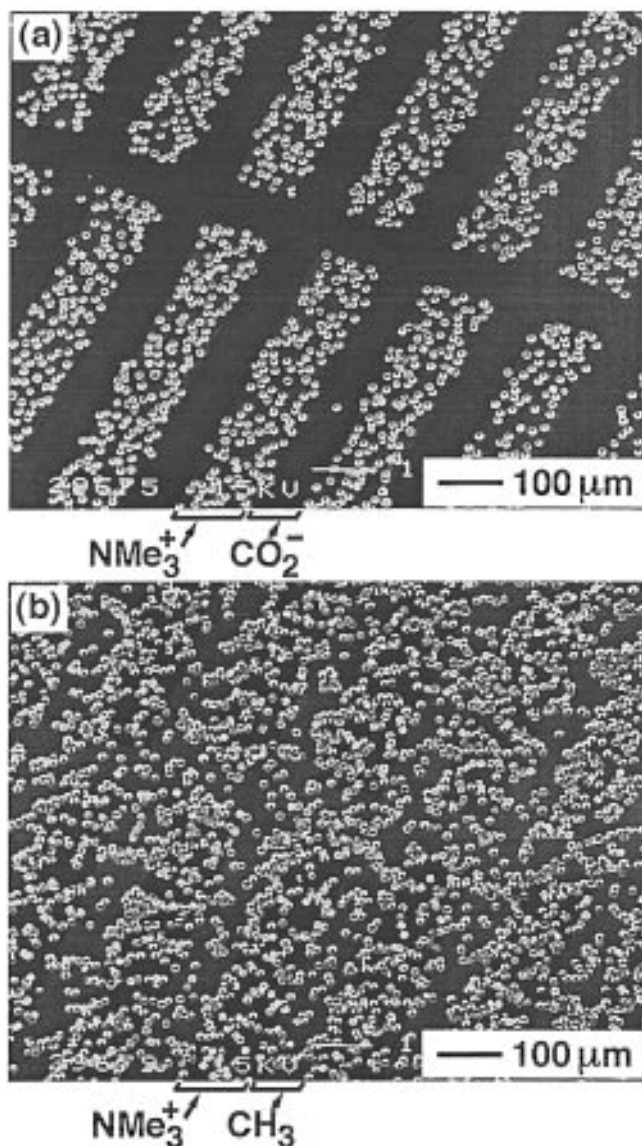


**Figure 4.** SEMs of  $\text{PO}_3\text{H}^-$ -terminated gold disks, assembled onto patterned gold. (a) Selective assembly: The gold surface was stamped with  $\text{HS}(\text{CH}_2)_{15}\text{COOH}$  (1 min), washed with  $1\text{ mM HS}(\text{CH}_2)_{11}\text{NMe}_3^+$  (30 s), and then rinsed with  $1\% \text{ HCl/EtOH}$  (10 s). The gold disks did not stick on  $\text{COOH}$ -terminated regions. (b) Defective assembly: The gold surface was stamped with  $\text{HS}(\text{CH}_2)_{15}\text{CH}_3$  (1 min), washed with  $1\text{ mM HS}(\text{CH}_2)_{11}\text{NMe}_3^+$  (30 s), and rinsed with  $1\% \text{ HCl/EtOH}$  (10 s). Assembly resulted in nonselective deposition; disks stuck on the supposedly nonstick Me-terminated regions.

charged particles. With careful stamping technique and appropriate choice of solvent to assemble from, it is possible to achieve patterned assemblies over  $\sim 1\text{ cm}^2$  areas. However, these assemblies lack in-plane ordering, presumably because the charged objects cannot slide laterally on the surface of the wafer once they are adsorbed. This lack of order limits the potential for complex self-assembly based solely on electrostatic interactions without designing additional features into the surface to allow equilibration and lateral ordering. We have achieved the required lateral mobility in self-assembly driven by capillary forces at a fluid–fluid interface,<sup>8,9</sup> and we believe a combination of these two approaches—electrostatics and capillary forces—will lead to ordered assemblies at the micrometer scale.

### Experimental Section

**Materials.** Hexadecanethiol, hexadimethrine bromide, and sodium poly(vinylsulfonate) were used as received from Aldrich.

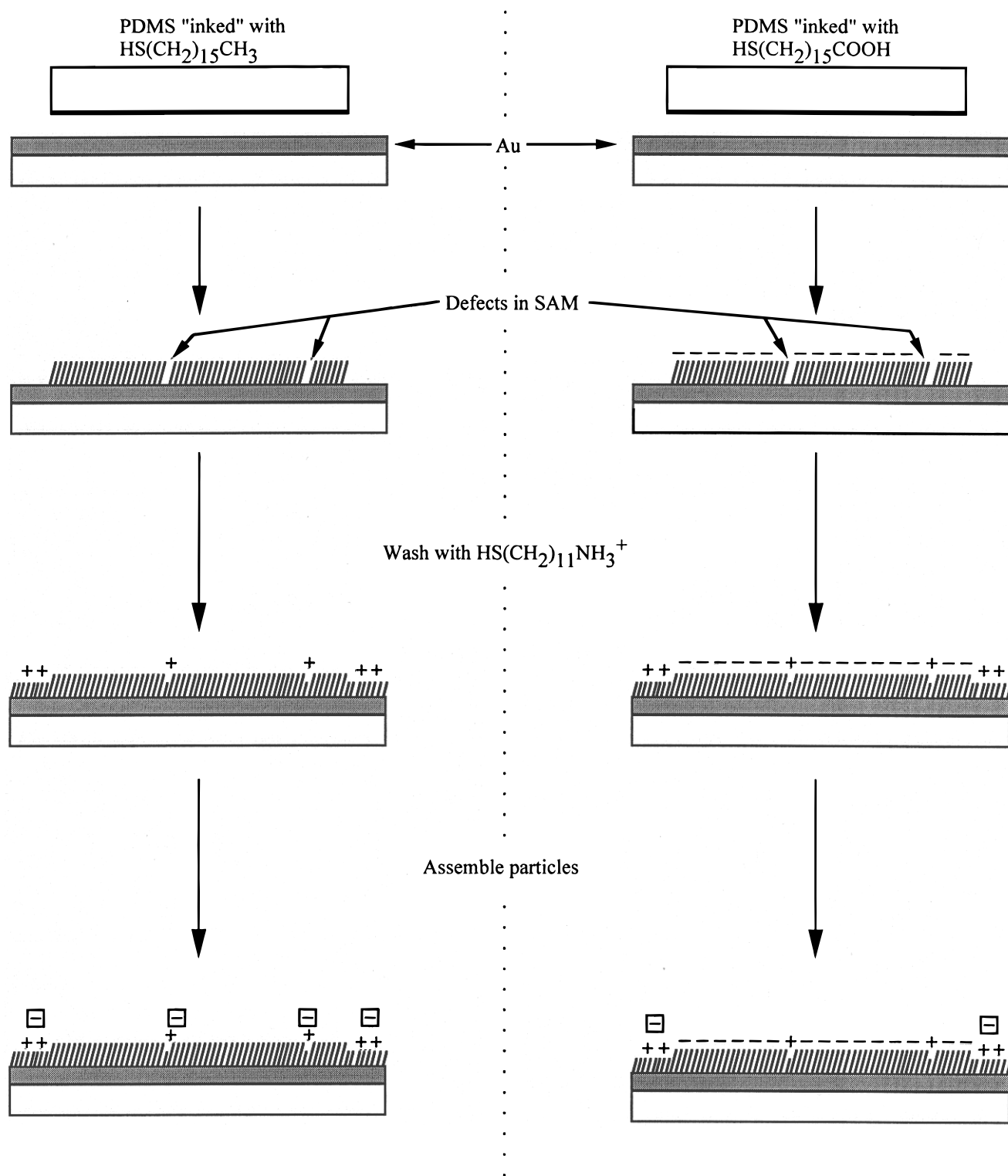


**Figure 5.** Schematic diagram comparing assembly on gold stamped with  $\text{HS}(\text{CH}_2)_{15}\text{CH}_3$  and assembly on gold stamped with  $\text{HS}(\text{CH}_2)_{15}\text{COOH}$ .

The acidic thiols  $\text{HS}(\text{CH}_2)_{15}\text{COOH}$  and  $\text{HS}(\text{CH}_2)_{11}\text{PO}_3\text{H}_2$  were synthesized according to published procedures.<sup>17</sup> *1H,1H,2H,2H*-tridecafluoro-1-octanethiol was a gift from Dr. Nandan Rao (du Pont). 1-Mercaptoundec-11-ylhexaethylene glycol was available from previous studies.<sup>18</sup> Gold sulfite plating solution (TG-25E, Technic Inc.) was plated at current densities of 1–5 mA/cm<sup>2</sup> and solution temperatures of 45–60 °C.

Gold substrates were made by evaporating 20–200 nm of gold, with 1–5 nm of titanium as adhesion promoter, onto polished

silicon wafers (Silicon Sense). Before use, all gold substrates were thoroughly washed with water and ethanol and cleaned in a hydrogen plasma.

**(11-Mercaptoundecyl)ammonium Chloride.** *N*-(10-Undecenyl)phthalimide. Potassium phthalimide (18.5 g, 100 mmol) and 10-undecenyl bromide (28 g, 120 mmol) were heated to reflux in DMF (100 mL) for 20 h. The cooled mixture was diluted with H<sub>2</sub>O and extracted twice with Et<sub>2</sub>O. The organic phase was washed with H<sub>2</sub>O, dried over Na<sub>2</sub>SO<sub>4</sub>, and evaporated to dryness.

(17) Lee, T. R.; Carey, R. I.; Biebuyck, H. A.; Whitesides, G. M. *Langmuir* **1994**, *10*, 741–749.

(18) Pale-Grosdemange, C.; Simon, E. S.; Prime, K. L.; Whitesides, G. M. *J. Am. Chem. Soc.* **1991**, *113*, 12–20.

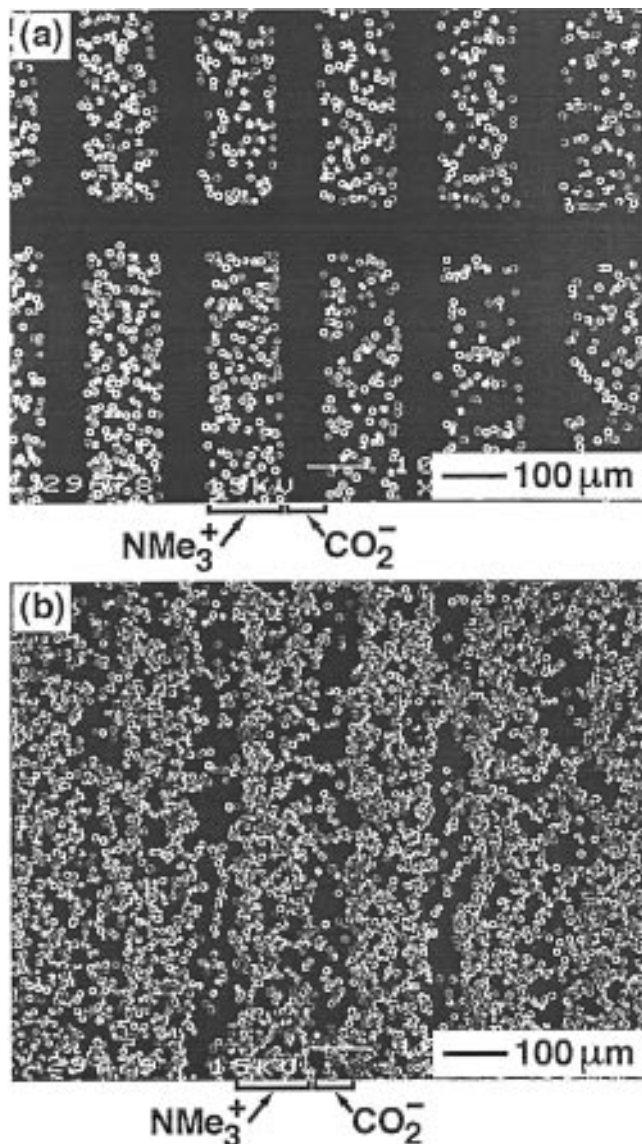


**Figure 6.** SEMs of  $\text{PO}_3\text{H}^-$ -terminated gold disks, assembled onto patterned gold. Gold wafers were patterned with  $\text{HS}-(\text{CH}_2)_{15}\text{COOH}$  and washed with 1 mM  $\text{HS}(\text{CH}_2)_{11}\text{NMe}_3^+$  and 1%  $\text{HCl}/\text{EtOH}$ . (a) Assembly in ethanol was selective. (b) Assembly in water was not selective.

Two crystallizations from MeOH (100 mL) yielded 23.7 g of off-white powder (79%). NMR ( $\text{CDCl}_3$ ): 1.21–1.42 (m, 12 H,  $\text{CH}_2$ ), 1.58–1.75 (m, 2 H,  $\text{CH}_2\text{CH}_2\text{N}$ ), 1.97–2.08 (m, 2 H,  $\text{CH}_2\text{CH}=\text{CH}_2$ ), 3.68 (t, 8 Hz, 2 H,  $\text{CH}_2\text{N}$ ), 4.88–5.04 (m, 2 H,  $\text{CH}=\text{CH}_2$ ), 5.72–5.91 (m, 1 H,  $\text{CH}=\text{CH}_2$ ), 7.67–7.90 (m, 4 H, arom.). *N*-(11-Thioacetylundecyl)phthalimide: *N*-(10-Undecenyl)phthalimide (23.7 g, 79 mmol) and thioacetic acid (20 mL, 280 mmol) were irradiated in  $\text{CH}_2\text{Cl}_2$  (100 mL) for 16 h. The volatiles were removed in vacuum, and the residue was crystallized twice from MeOH (100 mL each). Yield: 27.0 g (91%). NMR ( $\text{CDCl}_3$ ): 1.16–1.42 (m, 14 H,  $\text{CH}_2$ ), 1.47–1.61 (m, 2 H,  $\text{CH}_2\text{CH}_2\text{SAc}$ ), 1.61–1.74 (m, 2 H,  $\text{CH}_2\text{CH}_2\text{N}$ ), 2.32 (s, 3 H, Ac), 2.85 (t, 8 Hz, 2 H,  $\text{CH}_2\text{SAc}$ ), 3.68 (t, 8 Hz, 2 H,  $\text{CH}_2\text{N}$ ), 7.65–7.88 (m, 4 H, arom.). (11-Mercaptoundecyl)ammonium Chloride: *N*-(11-Thioacetylundecyl)phthalimide (13.5 g, 36 mmol) was heated with  $\text{H}_2\text{NNH}_2$  (4.0 mL, 125 mmol) in MeOH (125 mL) for 3 h. After removal of the volatiles, the residue was extracted with dilute HCl and then dried and extracted with  $\text{CH}_2\text{Cl}_2/\text{MeOH}$  (10:1). The organic extract was evaporated to dryness and the residue crystallized twice from  $\text{CH}_2\text{Cl}_2$  under addition of a minimal amount of MeOH, yielding 6.0 g of white crystals (82%). NMR (DMSO): 1.20–1.42 (m, 16 H,  $\text{CH}_2$ ), 1.46–1.62 (m, 2 H,  $\text{CH}_2\text{CH}_2\text{NH}_3^+$ ), 2.28 (d, 8 Hz, 1 H, SH), 2.44 (q, 8 Hz, 2 H,  $\text{CH}_2\text{SH}$ ), 2.65–2.81 (m, 2 H,  $\text{CH}_2\text{NH}_3^+$ ), 8.06 (s br, 3 H,  $\text{NH}_3^+$ ). MS (FAB): 204 (100%,  $\text{M}^+$ ), 170 (8%,  $\text{M}^+ - \text{H}_2\text{S}$ ).

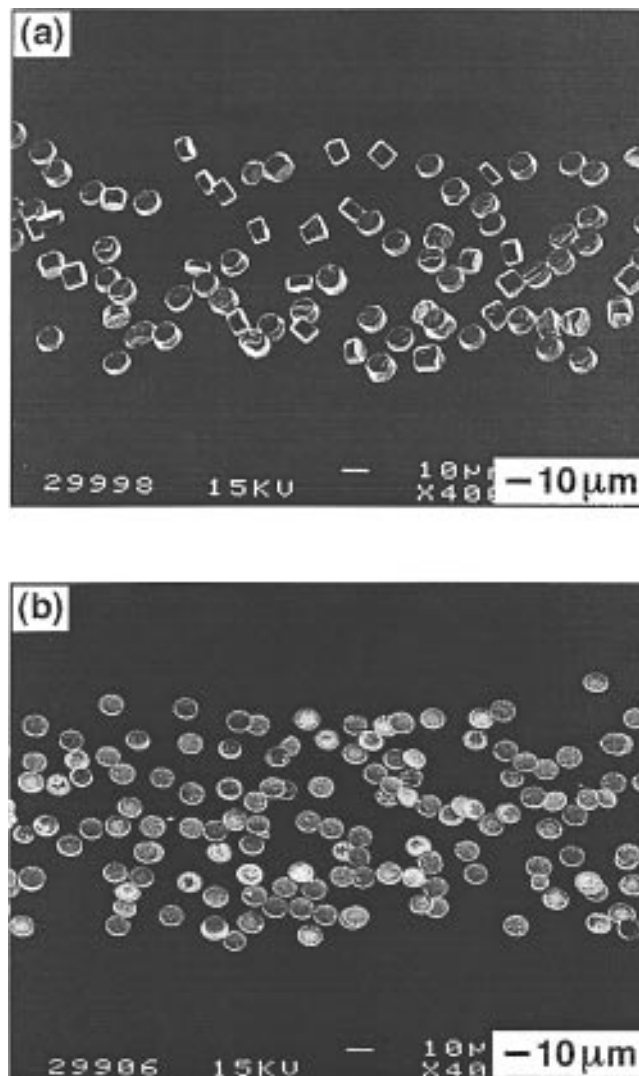


**Figure 7.** SEMs of  $\text{PO}_3\text{H}^-$ -terminated gold disks, assembled onto patterned gold. Gold wafers were patterned with  $\text{HS}-(\text{CH}_2)_{15}\text{COOH}$  and washed with 1 mM  $\text{HS}(\text{CH}_2)_{11}\text{NMe}_3^+$  and 1%  $\text{HCl}/\text{EtOH}$ . (a) Disks with an aspect ratio near 1:1 did not overlap each other. (b) Disks with an aspect ratio of  $\sim 1:15$  overlapped occasionally.

***N,N*-Dimethyl(11-mercaptoundecyl)ammonium Chloride.** 11-Thioacetylundecyl Bromide: A mixture of 10-undecenyl bromide (11.7 g, 50 mmol) and thioacetic acid (25 mL, 330 mmol) was irradiated for 16 h, and then excess thioacetic acid was removed *in vacuo*. The residue was the pure product in essentially quantitative yield. NMR ( $\text{CDCl}_3$ ): 1.22–1.49 (m, 14 H,  $\text{CH}_2$ ), 1.50–1.63 (m, 2 H,  $\text{CH}_2\text{CH}_2\text{SAc}$ ), 1.78–1.92 (m, 2 H,  $\text{CH}_2\text{CH}_2\text{Br}$ ), 2.33 (s, 3 H, Ac), 2.85 (t, 8 Hz, 2 H,  $\text{CH}_2\text{SAc}$ ), 3.42 (t, 8 Hz, 2 H,  $\text{CH}_2\text{Br}$ ). *N,N*-Dimethyl(11-mercaptoundecyl)ammonium Chloride: 11-Thioacetylundecyl bromide (4.6 g, 15 mmol) was added slowly (6 h) to a solution of dimethylamine in THF (2 M, 200 mmol) at 0 °C under vigorous stirring. After continued stirring for 24 h, the volatiles were removed *in vacuo*, and the residue was chromatographed with  $\text{CH}_2\text{Cl}_2/\text{MeOH}/\text{AcOH}$  (89:10:1) on silica. The product fraction was concentrated, taken up in dilute aqueous HCl, and concentrated again. This procedure was repeated several times, with a final lyophilization. White powder (3.1 g, 78 mmol). NMR ( $\text{CD}_3\text{OD}$ ): 1.23–1.49 (m, 14 H,  $\text{CH}_2$ ), 1.60–1.79 (m, 4 H,  $\text{CH}_2\text{CH}_2\text{SH} + \text{CH}_2\text{CH}_2\text{NMe}_2^+$ ), 2.50 (t, 8 Hz, 2 H,  $\text{CH}_2\text{SH}$ ), 2.86 (s, 6 H,  $\text{NMe}_2^+$ ), 3.03–3.14 (m, 2 H,  $\text{CH}_2\text{NMe}_3^+$ ), 4.88 (s, SH +  $\text{NH}^+$ ). MS (FAB): 246 (100%).

***N,N*-Dimethyl(11-mercaptoundecyl)amine.** Treatment of 50% EtOH solutions of *N,N*-dimethyl(11-mercaptoundecyl)ammonium chloride with Amberlite IRA-68 and lyophilization of the eluates resulted in liberation of the free amine as a colorless, air-sensitive liquid. NMR ( $\text{CDCl}_3$ ): 1.23–1.54 (m, 16 H,  $\text{CH}_2$ ),

1.55–1.68 (m, 2 H,  $\text{CH}_2\text{CH}_2\text{SH}$ ), 2.24 (s, 6 H,  $\text{NHMe}_2^+$ ), 2.23–2.32 (m, 2 H,  $\text{CH}_2\text{SH}$ ), 2.48–2.57 (m, 2 H,  $\text{CH}_2\text{NHMe}_2^+$ ).

***N,N,N*-Trimethyl(11-mercaptoundecyl)ammonium Chloride.** *N,N,N*-Trimethyl-10-undecenylammonium bromide: 10-Undecenyl bromide (12.5 mL, 52 mmol) was added at room temperature to a solution of  $\text{NMe}_3$  (~10 g, 170 mmol) in MeOH (50 mL) and stirred for 2 days. Removal of the volatiles, dissolution in  $\text{CH}_2\text{Cl}_2$  (~30 mL), and precipitation with hexanes (500 mL) yielded 15 g of colorless solid (99%). NMR ( $\text{CD}_3\text{OD}$ ): 1.23–1.47 (m, 12 H,  $\text{CH}_2$ ), 1.70–1.83 (m, 2 H,  $\text{CH}_2\text{CH}_2\text{N}^+$ ), 1.96–2.08 (m, 2 H,  $\text{CH}_2\text{CH}=\text{CH}_2$ ), 3.09 (s, 9 H,  $\text{NMe}_3^+$ ), 3.25–3.38 (m, 2 H,  $\text{CH}_2\text{N}^+$ ), 4.90–5.04 (m, 2 H,  $\text{CH}=\text{CH}_2$ ), 5.72–5.91 (m, 1 H,  $\text{CH}=\text{CH}_2$ ). *N,N,N*-Trimethyl(11-mercaptoundecyl)ammonium Chloride: A solution of *N,N,N*-trimethyl(10-undecenyl)ammonium bromide (2.92 g, 10 mmol) and thioacetic acid (2 mL, 26 mmol) in  $\text{CH}_2\text{Cl}_2$  (20 mL) was irradiated for 6 h. The volatiles were removed *in vacuo*, the residue was titrated several times with  $\text{Et}_2\text{O}$  and—after drying—refluxed in 10% HCl (20 mL) for 1 h. After removal of the acid *in vacuo*, the solid was crystallized from  $\text{H}_2\text{O}$  under  $\text{N}_2$  in the presence of decolorizing carbon. White solid (2.22 g, 79%). NMR ( $\text{D}_2\text{O}$ ): 1.24–1.49 (m, 14 H,  $\text{CH}_2$ ), 1.53–1.66 (m, 2 H,  $\text{CH}_2\text{CH}_2\text{SH}$ ), 1.67–1.84 (m, 2 H,  $\text{CH}_2\text{CH}_2\text{NMe}_3^+$ ), 2.52 (t, 8 Hz, 2 H,  $\text{CH}_2\text{SH}$ ), 3.12 (s, 9 H,  $\text{NMe}_3^+$ ), 3.30–3.41 (m, 2 H,  $\text{CH}_2\text{NMe}_3^+$ ). MS (FAB): 246 (100%), high res.: 246.2255.

**(11-Mercaptoundecyl)amidinium Chloride.** *10*-Undecenyl Cyanide: A mixture of 10-undecenyl bromide (24 mL, 100 mmol) and KCN (7.8 g, 120 mmol) in diethylene glycol (100 mL) was heated to 140 °C within 1 h. The cold mixture was diluted with  $\text{H}_2\text{O}$  and extracted with hexane. After removal of the solvent, the residue was treated with 50%  $\text{H}_2\text{SO}_4$  for 10 min, then extracted with hexane, washed with dilute brine, and concentrated. The remaining oil was distilled at 90 °C/0.1 kPa to yield a colorless oil (12.5 g, 70%). NMR ( $\text{CDCl}_3$ ): 1.18–1.51 (m, 12 H,  $\text{CH}_2$ ), 1.58–1.71 (m, 2 H,  $\text{CH}_2\text{CH}_2\text{CN}$ ), 2.00–2.10 (m, 2 H,  $\text{CH}_2\text{CH}=\text{CH}_2$ ), 2.33 (t, 8 Hz, 2 H,  $\text{CH}_2\text{CN}$ ), 4.90–5.04 (m, 2 H,  $\text{CH}=\text{CH}_2$ ), 5.72–5.91 (m, 1 H,  $\text{CH}=\text{CH}_2$ ). *10*-Undecenylamidinium Chloride: A solution of 10-undecenyl cyanide (4.48 g, 25 mmol) and EtOH (1.15 g, 25 mmol) in  $\text{Et}_2\text{O}$  (50 mL) was saturated with HCl gas at 0 °C and then stirred at room

temperature for 16 h. The volatiles were removed *in vacuo* before a saturated solution of  $\text{NH}_3$  in EtOH (50 mL) was added cautiously, and the resulting mixture was stirred for 2 days. The volatiles were removed *in vacuo* and the product was extracted into  $\text{CH}_2\text{Cl}_2$ . Most of the solvent was removed before petroleum ether (80 mL) was added to precipitate a colorless solid (4.94 g, 85%). NMR ( $\text{CDCl}_3$ ): 1.20–1.43 (m, 12 H,  $\text{CH}_2$ ), 1.64–1.81 (m, 2 H,  $\text{CH}_2\text{CH}_2\text{CN}$ ), 1.96–2.07 (m, 2 H,  $\text{CH}_2\text{CH}=\text{CH}_2$ ), 2.52–2.63 (m, 2 H,  $\text{CH}_2\text{C}(\text{NH}_2)_2^+$ ), 4.88–5.00 (m, 2 H,  $\text{CH}=\text{CH}_2$ ), 5.71–5.85 (m, 1 H,  $\text{CH}=\text{CH}_2$ ), 8.59 + 8.73 (2 s br, 4 H,  $\text{C}(\text{NH}_2)_2^+$ ). *(11-Mercaptoundecyl)amidinium Chloride*: A solution of 10-undecenylamidinium chloride (1.42 g, 6.0 mmol) and thioacetic acid (2 mL, 26 mmol) in  $\text{CH}_2\text{Cl}_2$  (20 mL) was irradiated for 7 h. The volatiles were removed *in vacuo*, the residue was titrated several times with  $\text{Et}_2\text{O}$  and—after drying—refluxed in 10% HCl (20 mL) for 1 h. The reaction mixture was lyophilized, the remaining solid dissolved in  $\text{CHCl}_3$  (5 mL), filtered, and precipitated with  $\text{Et}_2\text{O}$  (90 mL). White, hygroscopic solid (1.36 g, 84%). NMR ( $\text{CDCl}_3$ ): 1.15–1.55 (m, 18 H,  $\text{CH}_2$ ), 1.62–1.85 (m, 2 H,  $\text{CH}_2\text{C}(\text{NH}_2)_2^+$ ), 2.18 (s br, 1 H, SH), 2.45–2.65 (m, 2 H,  $\text{CH}_2\text{SH}$ ), 8.47 + 8.83 (2 s br, 4 H,  $\text{C}(\text{NH}_2)_2^+$ ). MS (FAB): 233 (100%), 231 (75%,  $\text{M}^+$ ), 197 (68%,  $\text{M}^+ - \text{SH}$ ), high res.: 231.1895.

**Acknowledgment.** This work was supported by NSF (CHE-9122331) and ONR/DARPA. We thank Andrew Black, Milan Mrksich, and Younan Xia for useful discussions, Yuanchang Lu for assistance with SEM, Stephen Shepard for assistance with photolithography, Lyle Isaacs for assistance with NMR, and Rebecca Jackman for experimental expertise. J.T. was supported by an predoctoral fellowship from NSF; A.T. thanks the Deutsche Forschungsgemeinschaft for a research grant. This work made use of MRSEC Shared Facilities supported by NSF (DMR-9400396), Mass Spectrometry Facilities supported by NSF (CHE-9020043), and NIH (S10-RR06716), and NMR facilities supported by NIH (S10-RR04870-01).

LA970454I